

Evidence for cospatial optical and radio polarized emission in active galactic nuclei

Denise C. Gabuzda,^{1*} Elizaveta A. Rastorgueva,^{2,3} Paul S. Smith⁴
and Shane P. O’Sullivan¹

¹*Department of Physics, University College Cork, Cork, Ireland*

²*Tuorla Observatory, Väisäläntie 20, FI-21500 Piikkiö, Finland*

³*Astro Space Center, Lebedev Physical Institute, 84/32 Profsoyuznaya St., Moscow 117 997, Russia*

⁴*Steward Observatory, The University of Arizona, Tucson, AZ, 85721 USA*

Accepted 2006 April 10. Received 2006 April 7; in original form 2006 January 20

ABSTRACT

We investigate the relationship between the optical and radio emission of active galactic nuclei (AGN) by analysing optical and 15+22+43 GHz Very Long Baseline Array (VLBA) polarization observations simultaneous to within a day for 11 BL Lacertae (BL Lac) objects and the blazar 3C279. We have determined and corrected for the Faraday rotation measures in the very long baseline interferometry (VLBI) cores, enabling us to compare the intrinsic (zero-wavelength) VLBI-core polarization angles and the optical polarization angles χ_{opt} . A clear alignment between these two angles emerges in the transition toward higher radio frequencies, and a prominent peak at 0° is visible in the distribution of $|\chi_{\text{opt}} - \chi_{43\text{GHz}}|$. This correlation implies that the magnetic-field orientations in the regions giving rise to the optical and radio polarization are the same, and can be easily understood if the radio and optical polarization are roughly cospatial. It is difficult to rule out the possibility that they arise in different regions in a straight jet with a uniform magnetic-field structure, but this seems less likely, since the VLBI jets of AGN are often bent on parsec-scales. This may suggest that much or all of the strong optical polarization in these sources arises in the inner radio jets, possibly associated with the formation and emergence of compact new VLBI components.

Key words: polarization – galaxies: active – galaxies: fields – galaxies: jets.

1 INTRODUCTION

The continua of radio-loud active galactic nuclei (AGN) are dominated by non-thermal (synchrotron) emission that is clearly associated with the relativistic jets in these objects, although the details of the jet structure and physics remain uncertain. BL Lacertae (BL Lac) objects are highly variable, appreciably polarized AGN that are observationally similar to radio-loud quasars, but display systematically weaker optical line emission. BL Lac objects and optically violently variable quasars are often collectively referred to as ‘blazars’.

Very long baseline interferometry (VLBI) polarization observations of BL Lac objects have shown a tendency for the polarization E vectors in the parsec-scale jets to be aligned with the local jet direction (Gabuzda, Pushkarev & Cawthorne 2000, and references therein). Since the jet emission is optically thin, this implies that the corresponding magnetic (B) field is orthogonal to the jet. This has been interpreted as evidence for relativistic shocks that enhance

the B -field component in the plane of compression, perpendicular to the direction of propagation of the shock (Laing 1980; Hughes, Aller & Aller 1989), although more recent analyses suggest that it may reflect the presence of toroidal or helical B fields associated with the jets (Gabuzda, Murray & Cronin 2004; Lyutikov, Pariev & Gabuzda 2005).

Although synchrotron radiation dominates over essentially the entire observed spectrum of blazars, it has usually been expected that there should be little correlation between observed properties in widely spaced wavebands, even if genuinely simultaneous measurements are compared. This is due in part to early attempts to search for optical–radio correlations based on integrated measurements that were unsuccessful or yielded ambiguous results (e.g. Kinman et al. 1974; Pomphrey et al. 1976; Rudnick et al. 1978). These results, together with the fact that the optical variations typically occur more rapidly than the radio variations, was taken as support for the idea that the optical emission is generated in a much smaller volume than the radio emission. It was therefore considered natural that there be no clear correlation between the high frequency and radio emission in AGN.

*E-mail: gabuzda@phys.ucc.ie

At the same time, in some inhomogeneous synchrotron source models for blazars, the radio and optical emission may be cospatial, depending on the model parameters considered. For example, Ghisellini, Maraschi & Treves (1985) present results for an inhomogeneous synchrotron self-Compton model for an emitting region with a jet-like geometry. They find that the radio and ultraviolet-optical-infrared (UVOIR) emission can come from the same, outer region of the jet, but only for some combinations of jet geometry and particle flow acceleration. For a different choice of jet geometry and particle flow, the UVOIR comes from one region (inner part of the jet), while the radio emission is produced primarily in a physically distinct (outer) region.

Therefore, there is a theoretical basis for the possibility that the UVOIR and radio jet emission are much more closely related than has usually been believed, and it is of interest to search for correlations between the emission of blazars in the UVOIR and radio. This task is complicated by the fact that most blazars are resolved at radio wavelengths only on milliarcsecond-scales, far beyond the resolving ability of UVOIR techniques, making it impossible to directly compare optical and radio images on the relevant scales. None the less, it is possible to use indirect methods to compare the emission at the two frequencies.

Indeed, a variety of data based on various indirect approaches suggest correlations between behaviour in widely separated wavebands. Indications of a connection between γ -ray outbursts and the ejection of VLBI components have been found (e.g. Pohl et al. 1995; Jorstad et al. 2001). Stirling et al. (2003) discovered a long-term tendency for the integrated 1-mm polarization position angle to remain aligned with the innermost 7-mm VLBI jet in BL Lac, even when this inner jet direction varied appreciably.

Gabuzda, Sitko & Smith (1996) analysed simultaneous optical polarization and 5-GHz VLBI polarization measurements for eight blazars, primarily BL Lac objects. In this case, the polarization of the radiation is essentially acting as a probe of the \mathbf{B} -field structures in the regions where the emission at the two wavelengths arises, potentially making it possible to identify the location of the optical emission within the VLBI structure. Although the results from that study were not conclusive due to the small number of objects considered, there were indications of a correlation between the polarization position angles in the optical χ_{opt} and in the VLBI core χ_{core} , with the two nearly always being either aligned or orthogonal. This trend was confirmed by an analysis of data for 15 blazars for which quasi-simultaneous optical and 5-GHz VLBI data were available (Gabuzda 2003).

Lister & Smith (2000) found a tendency for the optical polarization angle to lie along the direction of the 43/22-GHz VLBI jet in a number of quasars, with the tendency being somewhat stronger for more highly polarized quasars. They also found evidence for correlations between the degree of optical polarization and the VLBI-core polarization/luminosity, although this analysis was based on non-simultaneous optical and radio observations.

The bimodal behaviour shown by the difference in the simultaneously measured optical and 5-GHz core polarization angles can be understood if the optical and radio polarizations arises in regions with the same \mathbf{B} -field orientation, and the polarizations of the VLBI cores whose χ_{core} is aligned with and perpendicular to χ_{opt} are dominated by optically thin and optically thick emission regions, respectively. We present here the results of new simultaneous optical polarization data and VLBI polarization data for 12 blazars at 15, 22 and 43 GHz obtained to test this hypothesis.

2 OBSERVATIONS AND REDUCTION

2.1 Very Long Baseline Array (VLBA)

Polarization observations of 15 blazars also observed in the optical were carried out in two 24-h sessions starting at 06:00 UT on 2002 August 7 (henceforth Epoch A, six objects) and 06:00 UT on 2003 March 5 (Epoch B, nine objects) at 15, 22 and 43 GHz using the National Optical Astronomy Observatories (NRAO) Very Long Baseline Array (VLBA). In all cases, the sources were observed in a ‘snapshot’ mode, with roughly 8–10 several-minute scans of each object at each wavelength spread in time. The resulting coverage of the u - v plane was quite uniform. The data reduction and imaging were done with the NRAO Astronomical Imaging Processing System (AIPS) using standard techniques.

Simultaneous solutions for the instrumental polarizations and source polarizations for the compact sources 1156+295 (Epoch A) and OJ287 (Epoch B) were derived using the AIPS task LPCAL. The absolute calibration of the VLBI electric vector position angles (EVPAs) was determined using integrated polarization measurements from the NRAO VLA/VLBA Polarization and Flux Monitoring Database,¹ and requiring that the EVPA for the total VLBI polarization of a compact source coincide with the EVPA for the Very Large Array (VLA) core. The sources used for this purpose were 1749+096 and BL Lac for Epoch A (both observed with the VLA in B configuration on 2002 August 10), OJ287 and 3C279 (both observed with the VLA in A configuration on 2003 March 2) and 1538+149 (A configuration on 2003 March 16) for Epoch B. The short time intervals between the VLA and VLBA observations minimizes the possibility of variations in the source polarization between the dates of the VLA and VLBA observations. We estimate that these EVPA calibrations are accurate to within about 3°.

After the initial construction of the total intensity maps at 15, 22 and 43 GHz, we used the final self-calibrated visibility data to make maps of the distributions of the Stokes parameters Q and U at each frequency with matched resolutions corresponding to the 15-GHz beam. The Q and U maps were then used to construct the distributions of the polarized flux ($p = \sqrt{Q^2 + U^2}$) and polarization angle ($\chi = (1/2) \arctan(U/Q)$), as well as accompanying ‘noise maps’, using the AIPS task COMB. The formal uncertainties written in the output χ noise maps were calculated in COMB using the rms noise levels on the input Q and U maps. We then constructed rotation-measure maps for all the objects using the AIPS task RM, after first removing the contribution of the known foreground integrated Faraday rotation (Pushkarev 2001) at each frequency, so that any remaining non-zero rotation measure (RM) should be due to thermal plasma in the vicinity of the AGN.

2.2 Optical

The optical observations associated with Epoch A were obtained using the Steward Observatory 1.5-m telescope on Mt. Lemmon, Arizona, on 2002 August 8 spanning 05:00–10:00 UT. Thus, no more than one day separates these measurements from the radio observations. The ‘Two-Holer’ polarimeter (Sitko, Schmidt & Stein 1985) was used to measure the unfiltered ($\lambda_{\text{eff}} \sim 6000 \text{ \AA}$) linear polarization of the six blazars observed in Epoch A. The observations employed a 4-arcsec circular aperture, except for those of BL Lac,

¹ <http://www.aoc.nrao.edu/smyers/calibration/>

Table 1. Comparison of optical and VLBI polarizations.

Source	Epoch	m_{opt} (per cent)	χ_{opt}	χ_{15}	χ_{22}	χ_{43}	RM	χ_0	$\Delta\chi$
0823+033	B	5.4 ± 0.5	68 ± 3	30 ± 3	32 ± 4	41 ± 4		41 ± 4	27
OJ287 ^a	B	$19.3^{+0.5}_{-0.8}$	-10^{+10}_{-15}	3 ± 5	-10 ± 3	-7 ± 3		-7 ± 3	3
1147+245 ^a	B	$7.7^{+0.2}_{-0.2}$	59^{+2}_{-1}	26 ± 6	74 ± 3	74 ± 3		74 ± 3	15
3C279*	B	$24.6^{+1.1}_{-0.6}$	55^{+1}_{-1}	5 ± 4	35 ± 4	51 ± 4	-2360 ± 120	58 ± 2	3
1334 -127 ^a	B	$11.2^{+1.5}_{-0.8}$	48^{+8}_{-15}	48 ± 5	38 ± 3	45 ± 3		45 ± 3	3
1418+546	A	6.5 ± 0.4	23 ± 2	129 ± 5^b	123 ± 6^b	31 ± 4	410 ± 60	30 ± 1	7
1538+149 ^a	B	$20.4^{+0.6}_{-1.1}$	-32^{+4}_{-2}	-34 ± 3	-44 ± 3	-37 ± 3		-37 ± 3	5
1749+096	A	9.6 ± 0.4	1 ± 1	46 ± 4	18 ± 4	-10 ± 4	2860 ± 290	-16 ± 4	17
1823+568	A	9.4 ± 0.6	156 ± 2	37 ± 4	37 ± 4	30 ± 4	400 ± 95	30 ± 3	54
2131-021	A	2.4 ± 0.9	151 ± 12	78 ± 5	82 ± 4	80 ± 4		80 ± 4	71
2200+420	A	5.5 ± 0.2	5 ± 1	140 ± 4	63 ± 4	23 ± 5	6100 ± 370	4 ± 5	1
2254+074	A	13.8 ± 0.6	43 ± 1	64 ± 5	53 ± 5	48 ± 6	820 ± 90	45 ± 1	2

^a χ_{opt} and m_{opt} are interpolated to the median time of the VLBA observations. Differences between the interpolated and measured values are given by the subscripts and superscripts.

^bThese two angles rotated by 90° before fitting the RM (see Section 3).

where an 8-arcsec aperture was used. The data were acquired and reduced using the methods described by Smith et al. (1992). Table 1 lists the fractional optical polarizations (m_{opt} in per cent) and polarization position angles (χ_{opt}). The uncertainties are dominated by photon statistics (see Moore, Schmidt & West 1987).

Weather conditions at Kitt Peak were poor during the Epoch B radio observations, but *R*-band polarimetry was acquired at the Steward Observatory 2.3-m Bok Telescope on Kitt Peak, Arizona, on 2003 March 4 (eight sources) and 2003 March 7 (the same eight sources, plus 0823+033). These observations utilized the CCD Spectropolarimeter (SPOL; Schmidt, Stockman & Smith 1992). The March 4 data were obtained with SPOL in imaging mode, as described by Smith et al. (2002). An *R* filter was used with either 6- or 8-arcsec circular digital apertures. The March 7 SPOL observations were obtained in spectropolarimetric mode (see e.g. Smith et al. 2003). A slit width of 4.1 arcsec was used and the spectrum of polarization was averaged over 6000–7000 Å to be consistent with the earlier *R*-band imaging polarimetry. However, averaging over the broader wavelength range afforded by the spectropolarimetry leads to no significant differences from the results listed in Table 1. The formal observational uncertainties are dominated by photon statistics, as for the Two-Holer data. For the objects observed both before and after the radio observations, the m_{opt} and χ_{opt} values in Table 1 were interpolated to the median time of the Epoch B radio measurements for each source. The values given in the accompanying superscript and subscript are the differences between the interpolated values and the two available measurements.

3 RESULTS

Three of the 15 objects observed displayed VLBA-core polarization that was either weak or blended with strong polarization from the inner jet, making it difficult to isolate and estimate the core polarization angle, and could not be included in our analysis. The results for the remaining 12 objects are summarized in Table 1 and Fig. 1.

In six of the 12 objects, the wavelength dependence of the polarization angles in the core region was significant and consistent with the λ^2 law expected for Faraday rotation (e.g. Burn 1966). In all cases, the resulting RM distributions were smooth and continuous, sometimes showing a substantial enhancement toward the VLBI core—to several thousand rad m^{-2} in the cases of 3C279, 1749+096

and BL Lac (Table 1). In all six cases, we used the linear χ versus λ^2 relations to calculate the ‘zero-wavelength’ radio polarization angle χ_0 , in order to compare this value with the optical polarization angles χ_{opt} (Fig. 1, bottom right). The results are shown in Fig. 2.

In the case of 1418+546, the observed χ values for the core region at 15 and 22 GHz were roughly 90° from the value at 43 GHz, suggesting that the optically thick to thin transition occurred between 22 and 43 GHz. Thus, in order to estimate the core RM, we rotated the 15- and 22-GHz χ values by 90° before plotting χ versus λ^2 and fitting the RM (we could just as well have rotated the 43-GHz angles by 90° —it is important only that all three angles correspond to the same optical depth regime).

Of the remaining six objects, five had core χ values at the three frequencies that were equal within roughly 2σ or less. Although it was possible to obtain a formal fit for the RMs, the resulting values were equal to zero within $1-2\sigma$. We accordingly adopted the 43-GHz polarization angles for χ_0 , and there is no entry for the RM in Table 1. In the sixth object, 1147+245, the observed χ values at 22 and 43 GHz are equal (74°) within 1σ , while χ observed at 15 GHz is very different (26°). The good coincidence of the angles at the two higher frequencies suggests that the core RM is not very high; this large jump in the observed polarization angles between 22 and 15 GHz is presumably due to some combination of optical depth effects and possible contamination of the observed 15-GHz core χ value by polarized emission from the innermost jet.

Fig. 1 shows histograms of the difference between the optical and VLBA-core polarization angles at each of the three radio frequencies, $|\chi_{\text{opt}} - \chi_{\text{core}}|$. The χ_{core} values were determined as the mean within a 3×3 pixel area (i.e. nine elements) at the corresponding locations in the maps; the uncertainties in these angles were taken to be the rms deviation from these mean values added in quadrature to the overall 3° uncertainty in the absolute polarization-angle calibration.

While the 15-GHz distribution is quite flat, the 22-GHz distribution begins to show evidence for a predominance of sources for which χ_{opt} and χ_{core} are roughly aligned. This trend is continued by the 43-GHz distribution, which shows a clear peak corresponding to sources for which χ_{opt} and χ_{core} are aligned to within 10° . This trend reflects the decreasing influence of the core RMs on the observed χ_{core} with increasing frequency.

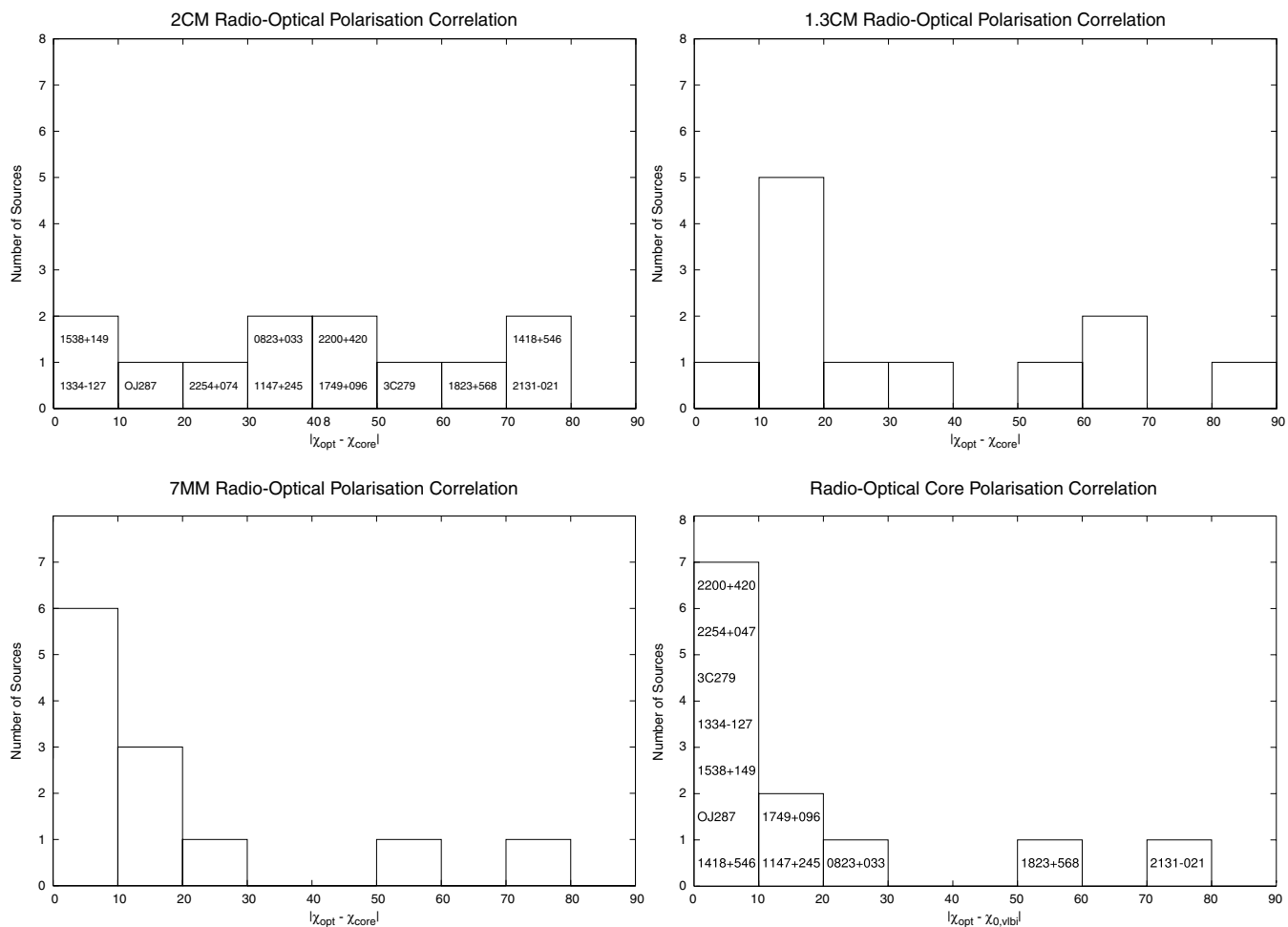


Figure 1. Histograms of $|\chi_{\text{opt}} - \chi_{\text{core}}|$ for the 15 GHz (top left), 22 GHz (top right) and 43 GHz (bottom left) VLBA radio cores. A histogram of the difference between χ_{opt} and the Faraday-corrected core polarization angle χ_0 is also shown (bottom right).

The bottom right histogram in Fig. 1 shows the distribution of $|\chi_{\text{opt}} - \chi_0|$, where χ_0 is the ‘zero-wavelength’ radio-core polarization angle. This looks very similar to the 43-GHz distribution, but shows a slightly sharper peak corresponding to sources with aligned χ_{opt} and χ_0 . These two angles are aligned to within 10° in seven of the 12 sources, suggesting that we have revealed a strong correlation between the optical polarization and the VLBA-core polarization of these blazars. Note that the $|\chi_{\text{opt}} - \chi_0|$ histogram also shows that the optical polarization angles did not vary greatly between the times of the radio and optical measurements: substantial variability in either the optical or radio measurements on time-scales of the order of a day would easily destroy the strong correlation observed.

4 DISCUSSION

4.1 The optical and VLBI-core polarization angles

A Kolmogorov–Smirnov test comparing the histogram in Fig. 1 with a uniform (flat) distribution indicates that the formal probability that the observed distribution is uniform is about 3.5 per cent. Note, however, that this test is limited by the small size of our sample; for example, if essentially the same distribution were observed for a sample about three times larger, the probability that it is uniform would fall to about 0.25 per cent. Thus, coordinated optical and

VLBA observations of additional blazars should be able to help clarify the statistical significance of this correlation.

As indicated above, we take the $\sim 90^\circ$ jump in the core polarization angles for 1418+546 between 22 and 43 GHz to demonstrate that the core is predominantly optically thick at 22 GHz but optically thin at 43 GHz. Thus, the χ_{core} value jumps from nearly perpendicular to nearly aligned with χ_{opt} in the transition from the optically thick to the optically thin regime, precisely as expected if the bimodal behaviour of $|\chi_{\text{opt}} - \chi_{\text{core}}|$ observed earlier at 5 GHz is due to the presence in the sample of objects with both optically thin ($\chi_{\text{core}} \parallel \chi_{\text{opt}}$) and optically thick ($\chi_{\text{core}} \perp \chi_{\text{opt}}$) cores. In this framework, it appears that the core of 2131–021, the only object with $\chi_{43\text{GHz}}$ roughly orthogonal to χ_{opt} , is still optically thick even at this high frequency (note, however, that this object was not optically highly polarized during Epoch A, and χ_{opt} is not as well constrained as for the other blazars).

The jet \mathbf{B} fields of BL Lac objects tend to be orthogonal to the local VLBI jet direction (Gabuzda et al. 2000, and references therein). For the seven of the 10 sources with $|\chi_{\text{opt}} - \chi_0| < 30^\circ$, the direction of $\chi_{\text{opt}}(\chi_0)$ coincides with the position angle of the innermost jet. In addition, χ_{opt} for 2131–021 is aligned with the inner jet of that source. Thus, the optical polarization is apparently emitted by regions where \mathbf{B} is orthogonal to the jet, indicating that this tendency is preserved on scales smaller than the resolution of our 43-GHz

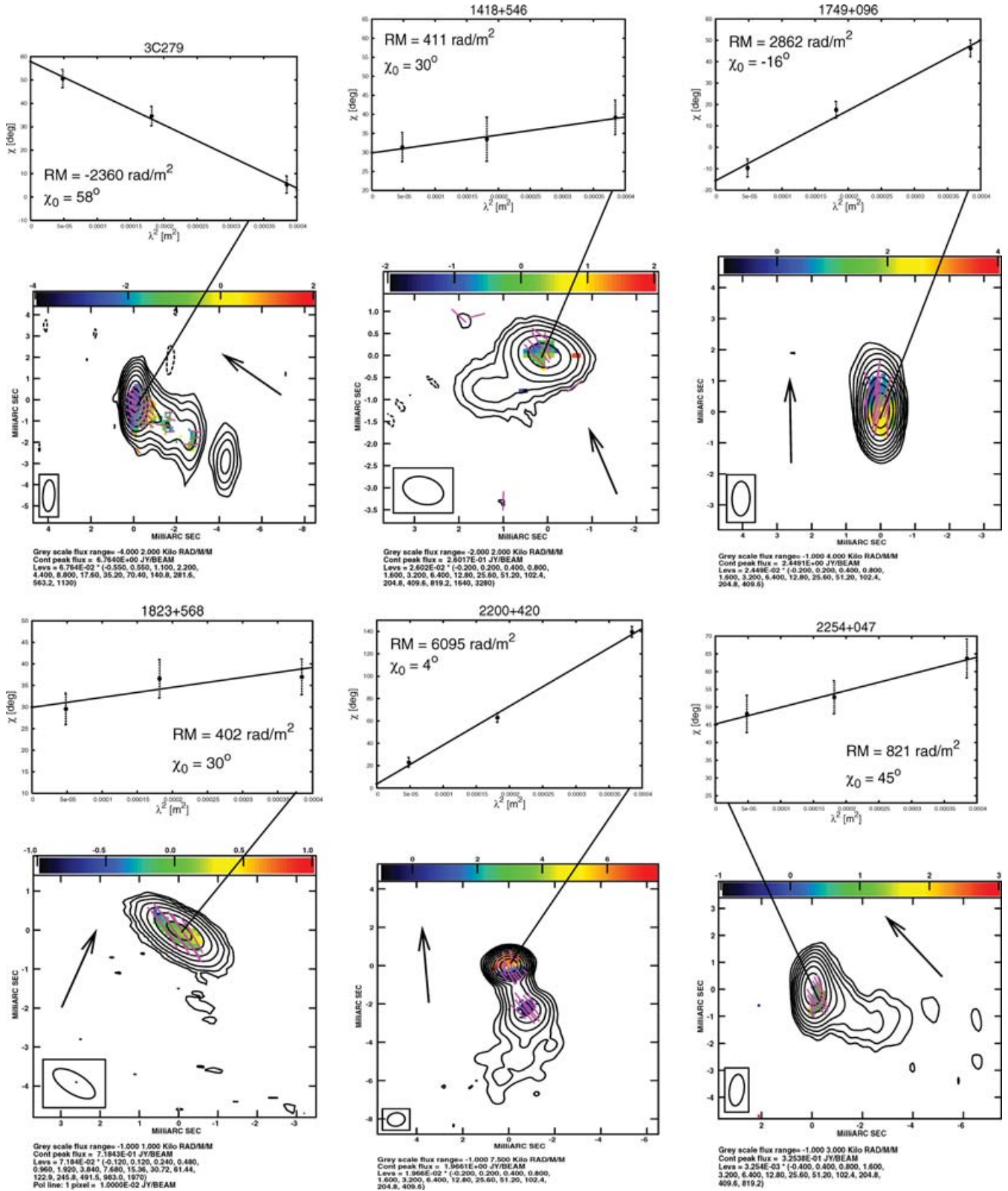


Figure 2. 43-GHz total intensity contours and the parsec-scale RM distribution in colour for 3C279 (top left), 1418+546 (top middle), 1749+096 (top right), 1823+568 (bottom left), 2200+420 (bottom middle) and 2254+074 (bottom right). The superposed polarization vectors χ_0 have been corrected for the parsec-scale RM distribution. The accompanying plots of the VLBA core χ values versus λ^2 clearly show the linear behaviour expected for Faraday rotation. The bold arrows next to the images show the orientation of the optical polarization.

images. At the same time, the presence of three sources with χ_{opt} and χ_0 aligned and with both oriented *orthogonal* to the innermost jet indicates that a sizable minority of sources have longitudinal \mathbf{B} fields on smaller scales than those we have sampled.

1823+568 displays an appreciable offset (54°) between χ_{opt} and χ_0 , with χ_0 aligned with the innermost VLBI jet. In this case, the optical and radio polarizations apparently arise in substantially different regions of the source; it may be that χ_{opt} bears some relation to the jet direction on scales much smaller than our resolution.

4.2 The core rotation measures

Previous core RM measurements are available for five of the six objects that displayed measurable core Faraday rotations. Previous measurements of the core RM of 3C279 at multiple frequencies near 15 and 8.4 GHz have yielded values ranging from -1280 rad m^{-2} to as low as about -100 rad m^{-2} (Zavala & Taylor 2001, 2003). The core RMs of 1749+096 (Zavala & Taylor 2004; Gabuzda & Pashchenko, in preparation), 1823+568 (Zavala & Taylor 2003; Gabuzda & Pashchenko, in preparation) and 2200+420 (Reynolds, Cawthorne & Gabuzda 2001; Zavala & Taylor 2003) measured at various combinations of frequencies between 15 and 5 GHz, all have magnitudes of about one to several hundred rad m^{-2} . In all these cases, the core RMs we have measured at 15–43 GHz are substantially higher than these values—by up to an order of magnitude for 1749+096 and 2200+420. The case of 1418+546 is less clear; depending on how the 5–15 GHz polarization angles are interpreted (allowing for possible optical depth effects and $n\pi$ ambiguities in χ), the corresponding VLBI core RM could equally plausibly be either +480 or -960 rad m^{-2} (Gabuzda & Pashchenko, in preparation), with the former being equal to the value in Table 1 to within the errors.

This comparison raises the question of the consistency of the results presented here with the previous results obtained at somewhat lower frequencies. The differences between the various sets of results for individual sources are sufficiently large, and the fits to λ^2 laws sufficiently good in both cases, that we can rule out the possibility that the large differences in the derived RMs are due to observational errors. One possibility is that at least some of the observed differences are due to intrinsic variability in the core RMs, as has been observed for 3C279 (Zavala & Taylor 2001, 2003). However, there is an alternative explanation for these results that does not require that the core RMs be variable: the difference in the resolutions of the various sets of observations. Since the early 1980s, it has been the standard view that the radio core of an AGN represents the optically thick ($\tau \simeq 1$) base of the approaching relativistic jet (e.g. Blandford & Königl 1979). This view is supported observationally by the fact that the spectra of the compact core components do, in fact, tend to be flat or inverted, rather than steep. However, the *observed* compact feature that would usually be referred to as the ‘VLBI core’ coincides with the *theoretical* concept of the core as the $\tau = 1$ surface of the VLBI jet only if the observations have sufficient resolution to isolate this optically thick region. If the beam size corresponding to a certain observation is appreciably larger than the size-scale of the $\tau = 1$ surface, the observed ‘VLBI core’ will in fact include emission from both the optically thick core and optically thin regions in the innermost VLBI jet.

The fact that the observed VLBI core contains both optically thick and optically thin regions will affect interpretation of both its spectrum and its polarization properties. In particular, the lower resolutions provided by observations at 8.4–15 or 5–15 GHz compared to observations at 15–43 GHz mean that the observed VLBI ‘cores’

at the lower frequencies will encompass more of the optically thin inner jet. This effect is also enhanced by the fact that this inner jet emission will be more prominent relative to the optically thick core emission at lower frequencies. Since the parsec-scale RM values show a clear tendency to fall off rather rapidly with distance from the core (Reynolds et al. 2001; Gabuzda & Chernetskii 2003; Zavala & Taylor 2003, and references therein), the lower frequency measurements of the ‘core’ RMs are more ‘contaminated’ by regions of the inner jet that have relatively low RMs. This provides a natural explanation for the higher RM values we have measured, compared to those obtained at somewhat lower frequencies. Another possible effect is the presence of separate regions in the core/innermost jet with RMs of opposite sign, leading to partial or complete cancellation of the RMs in lower resolution observations.

Such inhomogeneities in the RM distribution could be expected under some circumstances to lead to appreciable deviations from λ^2 behaviour in the lower resolution observations. It is interesting that the 8.1–15.2 GHz core polarization angles for 2200+420 measured by Zavala & Taylor (2003) do show substantial deviations, in particular, at their highest frequency, with these deviations being qualitatively consistent with the inferred RM becoming higher and positive at even higher frequencies. At the same time, no significant deviations are evident for the other three sources for which previous lower resolution observations are available. However, even if the observed core polarizations are effectively sums over regions with differing RM and spectral index, there could still be only negligible deviations from λ^2 behaviour for the polarization angles in practice if the contribution of a single relatively homogenous region dominates the observed core polarization. This may provide an explanation for the lack of deviations from linear behaviour in the RM graphs for these other three sources. The plausibility of our various possible interpretations of the higher core RMs implied our 15–43 GHz observations could be directly verified with VLBA observations spanning frequencies from 5 to 43 GHz within a single experiment.

This picture of the observed VLBI core as being comprised both optically thick and optically thin regions can also explain why evidence for correlations between χ_{opt} and χ_{core} emerged in our earlier comparisons of optical and 5-GHz polarization data, even though the local core RMs can be high and the 5-GHz core polarization angles were only corrected for the integrated (Galactic) RMs. Because of both the lower resolution and the increased prominence of the optically thin inner jet relative to the optically thick true core at 5 GHz, the observed ‘core’ polarization angles are much more dominated by the contribution of regions of low local RM.

5 CONCLUSION

We have found a striking correlation between the nearly simultaneously measured optical and high-frequency VLBI-core polarization angles, corrected for the observed Faraday rotation when appreciable. These two polarization angles are aligned to within 20° for nine of 12 compact AGN analysed. In a 10th object (0823+033), χ_{opt} and χ_0 are aligned to within 30° , and in another source (2131–021) they are perpendicular to each other to within 20° . This last case can be understood if these two angles are correlated, but the radio core remains optically thick at 43 GHz. Only one of the dozen AGN analysed does not give any hint of a relation between its optical and VLBI-core polarization angles (1823+568).

One possible explanation for the correlation we have revealed is that the optical and VLBI-core polarizations originate in the same or neighbouring regions in the source with very similar \mathbf{B} -field

orientations. However, it is difficult to rule out the possibility that they arise in different regions within a straight jet with a uniform \mathbf{B} -field structure. One piece of circumstantial evidence against this latter possibility is the fact that the VLBI jets of BL Lac objects and other blazars are often bent on parsec-scales (e.g. Kellermann et al. 1998; Zensus et al. 2002), and it would not be surprising if this tendency continued on subparsec-scales. However, it is not currently possible to firmly distinguish between these two scenarios. Further coordinated optical and VLBI observations may help elucidate this question. For example, is support for the cospatial interpretation provided via cases of well-aligned χ_{opt} and χ_{core} angles that are both at some arbitrary orientation relative to the 43-GHz VLBI jet? Are there cases when χ_{opt} is well aligned with χ_0 in the innermost VLBI jet, but not with χ_0 in the core? Observations of simultaneous rotations in aligned polarization angles in the optical and VLBI core would also support the hypothesis that the optical and VLBI-core emission regions were cospatial. Further observations may help shed light on this question, as well as give indications about whether correlations between χ_{opt} and χ_0 are equally common among different types of AGN.

In all but one source, χ_{opt} is either aligned with (eight objects) or orthogonal to (three objects) the innermost jet. This close relation between χ_{opt} and the VLBI jet direction clearly indicates that the optical polarization is associated with compact regions of the jets of these AGN. One possibility is that both the optical and compact radio-core polarization are dominated by the contribution of compact jet components as they are formed and emerge from the core. The fact that χ_{opt} and the associated optically thin χ_0 are both approximately aligned with the direction of the innermost jet in eight of the 12 sources suggests that the tendency for the jet \mathbf{B} fields of BL Lac objects to be orthogonal to the jet direction is preserved on scales appreciably smaller than our resolution. This would be quite natural if these orthogonal fields are associated with toroidal or helical \mathbf{B} fields that are organically related to the jets and their formation (e.g. Lyutikov et al. 2005, and references therein).

ACKNOWLEDGMENTS

PSS acknowledges support from NASA/JPL contract 1256424. The National Radio Astronomy Observatory is operated by Associated Universities, Inc., under cooperative agreement with the NSF. We thank the anonymous referee for promptly providing relevant, constructive comments that appreciably improved this paper.

REFERENCES

- Blandford R. D., Königl A., 1979, *ApJ*, 232, 34
 Burn B. J., 1966, *MNRAS*, 133, 67
 Gabuzda D. C., 2003, *Ap&SS*, 288, 39
 Gabuzda D. C., Chernetskii V. A., 2003, *MNRAS*, 339, 669
 Gabuzda D. C., Sitko M. L., Smith P. S., 1996, *AJ*, 112, 1877
 Gabuzda D. C., Pushkarev A. B., Cawthorne T. V., 2000, *MNRAS*, 319, 1109
 Gabuzda D. C., Murray É., Cronin P., 2004, *MNRAS*, 351, L89
 Ghisellini G., Maraschi L., Treves A., 1985, *A&A*, 146, 204
 Hughes P. A., Aller H. D., Aller M. A., 1989, *ApJ*, 341, 68
 Jorstad S. G., Marscher A. P., Mattox J. R., Aller M. F., Aller H. D., Wehrle A. E., Bloom S. D., 2001, *ApJ*, 556, 738
 Kellermann K. I., Vermeulen R. C., Zensus J. A., Cohen M. H., 1998, *AJ*, 115, 1295
 Kinman T. D., Wardle J. F. C., Conklin E. K., Andrew B. H., Harvey G. A., MacLeod J. M., Medd W. J., 1974, *AJ*, 79, 349
 Laing R., 1980, *MNRAS*, 193, 439
 Lister M. L., Smith P. S., 2000, *ApJ*, 541, 66
 Lyutikov M., Pariev V. I., Gabuzda D. C., 2005, *MNRAS*, 360, 869
 Moore R. L., Schmidt G. D., West S. C., 1987, *ApJ*, 314, 176
 Pohl M. et al., 1995, *A&A*, 303, 383
 Pomphrey R. B., Smith A. G., Leacock R. J., Olsson C. N., Scott R. L., Pollock J. T., Edwards P., 1976, *AJ*, 81, 489
 Pushkarev A. B., 2001, *Astron. Rep.*, 45, 667
 Reynolds C., Cawthorne T. V., Gabuzda D. C., 2001, *MNRAS*, 327, 1071
 Rudnick L., Owen F. N., Jones T. W., Puschell J. J., Stein W. A., 1978, *ApJ*, 225, L5
 Schmidt G. D., Stockman H. S., Smith P. S., 1992, *ApJ*, 398, L57
 Sitko M. L., Schmidt G. D., Stein W. A., 1985, *ApJS*, 59, 323
 Smith P. S., Hall P. B., Allen R. G., Sitko M. L., 1992, *ApJ*, 400, 115
 Smith P. S., Schmidt G. D., Hines D. C., Cutri R. M., Nelson B. O., 2002, *ApJ*, 569, 23
 Smith P. S., Schmidt G. D., Hines D. C., Foltz C. G., 2003, *ApJ*, 593, 676
 Stirling A. M. et al., 2003, *MNRAS*, 341, 405
 Zavala R., Taylor G. B., 2001, *ApJ*, 550, L147
 Zavala R., Taylor G. B., 2003, *ApJ*, 589, 126
 Zavala R., Taylor G. B., 2004, *ApJ*, 612, 749
 Zensus J. A., Ros E., Kellermann K. I., Cohen M. H., Vermeulen R. C., Kadler M., 2002, *AJ*, 124, 662

This paper has been typeset from a $\text{\TeX}/\text{\LaTeX}$ file prepared by the author.